Macromolecular Research, Vol. 16, No. 3, pp 204-211 (2008)

Platinum-Catalyzed and Ion-Selective Polystyrene Fibrous Membrane by Electrospinning and *In-Situ* Metallization Techniques

Seung-Hee Hong, Sun-Ae Lee, and Jae-Do Nam*

Department of Polymer Science and Engineering, Sungkyunkwan University, Suwon 440-746, Korea

Young-Kwan Lee

Department of Chemical Engineering, Sungkyunkwan University, Suwon 440-746, Korea

Tae-Sung Kim

School of Mechanical Engineeing, Sungkyunkwan University, Suwon 440-746, Korea

Sungho Won

Microelectronic Packaging R&D Center, Sungkyunkwan University, Suwon 440-746, Korea

Received July 31, 2007; Revised December 4, 2007

Abstract: A platinum-catalyzed polyelectrolyte porous membrane was prepared by solid-state compression of electrospun polystyrene (PS) fibers and *in-situ* metallization of counter-balanced ionic metal sources on the polymer surface. Using this ion-exchange metal-polymer composite system, fiber entangled pores were formed in the interstitial space of the fibers, which were surrounded by sulfonic acid sites (SO_3^-) to give a cation-selective polyelectrolyte porous bed with an ion exchange capacity (I_{EC}) of 3.0 meq/g and an ionic conductivity of 0.09 S/cm. The Pt loading was estimated to be 16.32 wt% from the SO_3^- ions on the surface of the sulfonated PS fibers, which interact with the cationic platinum complex, $Pt(NH_3)_4^{2-}$, at a ratio of 3:1 based on steric hindrance and the arrangement of interacting ions. This is in good agreement with the Pt loading of 15.82 wt% measured by inductively coupled plasma-optical emission spectroscopy (ICP-OES). The Pt-loaded sulfonated PS media showed an ionic conductivity of 0.32 S/cm. The *in-situ* metallized platinum provided a nano-sized and strongly-bound catalyst in robust porous media, which highlights its potential use in various electrochemical and catalytic systems.

Keywords: sulfonation, membrane, platinum, fuel cell.

Introduction

Polyelectrolyte and their metal composite systems have played a crucial role in the development of various electrochemical applications, such as fuel cells, supercapacitors, sensors, actuators, etc.[1-9] As one of the most significant applications in polyelectrolyte composite systems, the fuel cell is considered to be a promising alternative power source, because of its high energy efficiency and environment-friendly nature.[10-13] One of the most widely utilized and commercially available polyelectrolytes is the perfluorosulfonated polymer, of which the most well-known is Nafion.[14,15] While it has well-balanced properties such as chemical, electrochemical, and mechanical stability with high proton conductivity, the major drawback to the large-scale commercial use of Nafion is the cost issue.[16] Much effort has been made to develop new ion-selective systems such as poly(aryl ether ketone)s,[17] poly(ether sulfone)s,[18] and polyimides[19] for the purpose of replacing Nafion.

One of the most probable routes to a high-performance cost-effective polymer electrolyte may be the use of hydrocarbon polymers for the polymer backbones.[12] In hydrocarbon polymers, sulfonated PS may be a valid alternative to the very expensive Nafion. It has been reported that the ionic conductivity of homogeneously sulfonated PS is 0.086 S/cm[20], which is comparable to that of Nafion.[4,5] In addition, the membrane form of porous media prepared by the radiochemical grafting of styrene monomer on poly(vinylidene fluoride) porous films followed by sulfonation was reported to be 0.058 S/cm, which is comparable to that of Nafion, 0.053 S/cm.[21]

The polyelectrolyte porous systems made by these hydro-

*Corresponding Author. E-mail: jdnam@skku.edu

carbon polymers are highly porous and their pore size should be adjusted to allow cations to be exchanged. For example, a cross-linked, high density polyethylene porous membrane, which was filled with an acrylamide *tert*-butyl sulfonate sodium salt in the pores, mechanically prevented the excessive swelling of the filling polymer and thus reduced the methanol crossover in fuel cell applications.[22] Among the various methods of synthesizing porous membranes, the electrospinning method, in which the polymer solution is delivered through a nozzle under an electrical potential, gives rise to well developed porous media.[23] This method has been used for making various-sized porous structures.[24,25] It is considered that the porous media produced by the electrospun fibers may provide a suitable pore structure for use as a polyelectrolyte system in fuel cell applications. The pore size can be controlled by adjusting the degree of fiber compaction and fiber diameter, because porosity is naturally formed in the interstitial space of the mechanically-entangled electrospun fibers.

In direct methanol fuel cells (DMFCs), two distinct layers of the polyelectrolyte membrane and the catalyst layer may be integrated to reduce the methanol crossover by consuming the crossover methanol molecules in the presence of Pt metal particles in both the membrane and catalyst layer.[26] For example, Pt particles have been incorporated into polyelectrolyte membranes to reduce the methanol crossover,[27] which could improve the catalyst performance.[28] The self-assembled Pt nanoparticles on the polyelectrolyte Nafion surface inhibited the crossover by the catalytic recombination of the crossover H_2 or methanol with O_2 to improve the fuel cell performance,[29] where the 1.8-2 nm sized Pt particles were synthesized in the presence of poly(diallyldimethylammonium chloride, PDDA) stabilizers to give a self-assembled Pt-PDDA electrode. However, it should be mentioned that the self-assembly bonding between the metal and the organic surface is not strong enough to sustain against the external stresses commonly exerted in most engineering processes and, particularly, the electrostatic or hydrogen bonding forces can be easily broken in most electrolyte solutions.[30-32]

In our previous study, we reported that a strong bond can be formed between the polymer surface and the gold nanoparticles by the *in-situ* chemical reaction of a metal-ion complex in the vicinity of the charged polymer surface due to the soft nature of the metal (gold) ions and sulfur atoms.[33] A similar route was applied to achieve strong metal-polymer bonding[34-40] in the ion-exchange polymer metal composites (IPMC), which sustained its layered structure under a large amount of bending deformation.[41,42] In this *in-situ* direct metallization route, it is believed that the metal loading density and the final morphology of the metal/polymer composite are determined by the number of ion exchange sites formed on the polymer surface, which is an absolute measure of the reactive sites available for the ionic metal complex to be metallized.[34-40] Using this method, the nano-sized Pt particles may be formed on the electrospun PS fiber surfaces via the *in-situ* metallization to give a catalyst-incorporated polyelectrolyte porous system.

In this study, a PS solution was electrospun and sulfonated with chlorosulfonic acid followed by the compression molding to give a robust ion-selective porous membrane. The Pt nanoparticles were synthesized on the PS fiber surface by the ionic interaction of a cationic Pt complex with the anionic sulfonic groups to provide a Pt-catalyzed cation-selective porous bed.

Experimental

Amorphous polystyrene (M_w: 240,000), chlorosulfonic acid, *N*,*N*-dimethyl formamide (DMF), tetraamine platinum (II) nitrate ($Pt(NH_3)_4(NO_3)_2$), and sodium borohydride ($NaBH_4$) were purchased from Aldrich, and used without further purification.

PS solutions with different concentrations, viz. 20, 22, 24, 26, and 28 wt%, were prepared by dissolving PS in DMF. The PS solutions were stirred by a magnetic bar for 12 h at room temperature. The electrospinning set-up consisted of a syringe and a needle. The PS solutions were poured into a 10 mL syringe attached to a 22 mm diameter capillary tip, and delivered by a microsyringe pump.[24] The high potential electrode of the power supply (HYP-303D power supply, Han Young Co., Korea) was connected to a copper wire inserted into the PS solutions, and the ground electrode was connected to the collector, which was a metal collector wrapped with aluminum foil. The production rate was varied from 0.1 to 15 mL/h, and the tip-to-collector distance was fixed at 10 cm.

As shown in Scheme I, the prepared electrospun PS fibers were sulfonated using chlorosulfonic acid for a period of more than 30 min at room temperature (step I). After dipping the electrospun fibers in chlorosulfonic acid, the solution was mixed properly to exchange H^+ with SO_3^- and subsequently neutralized with ethyl alcohol. To prevent any damage being caused to the sulfonated PS fibers, they were washed very carefully in ethyl alcohol in an ice bath several times.[43] Then, they were removed from the bath, rinsed with deionized water, and kept in a vacuum oven at 40 °C overnight. The sulfonated PS fibers were compressed to create a membrane form by a roll-to-roll lamination process (Lami-art-320LSI, GMP Co., Korea) at 25-40 °C. The lamination process was repeated several times to reach a final film thickness of around 400 μm.

For the preparation of the Pt-loaded PS porous membrane, the sulfonated PS fibers were immersed in 0.1 mol $Pt(NH_3)_4(NO_3)_2$ solution for 2 h with stirring (step II in Scheme I) and subsequently reduced in 1 mol $NaBH_4$ solution at room temperature for 4 h (step III in Scheme I). The Pt metallization process (steps II and III in Scheme I) was conducted twice to reach the final Pt loading. After the

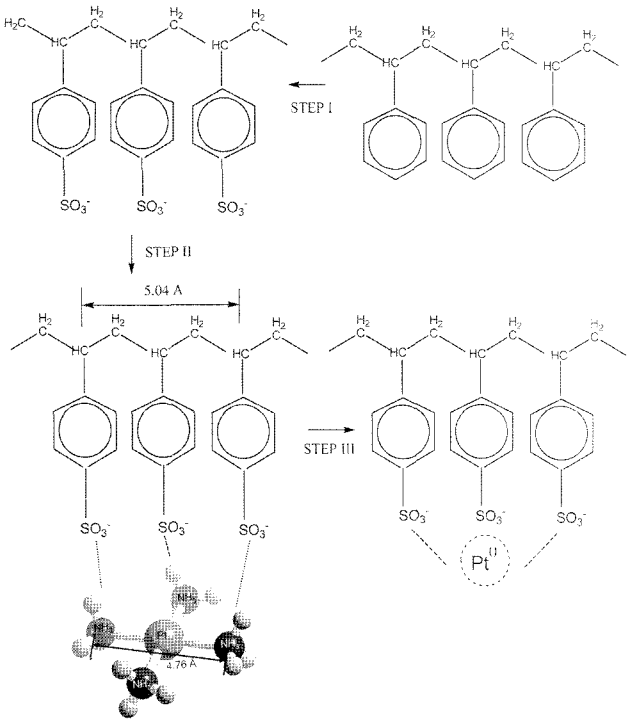

Scheme I. Preparation scheme of Pt-loaded PS membranes. Electrospun PS fibers are functionalized by chlorosulfonic acid (step I). Then $Pt(NH_3)_4^{2-}$ is adsorbed on the negatively charged PS fibers (step II), and subsequently reduced by $NaBH_4$ to give Pt nanoparticles on the electrospun PS fibers (step III).

reduction process, the Pt-loaded PS fibers were washed several times with deionized water to eliminate the excessive Pt ions. The Pt-loaded PS fibers were laminated by the roll-to-roll press as described earlier. The membrane porosity was 70 %, defined as the volume of the pores divided by the total volume of the porous film. The porosity was determined by equilibrating in water for 24 h in a closed container and determined gravimetrically from the difference in the weights and volumes of the dried samples and their wet counterparts.

For the measurement of the ion exchange capacity (I_{EC}, meq of SO_3H/g) by the acid-base titration method, the sulfonated PS fibers (preferably 0.5-1.0 g) were immersed in 50 mL of saturated sodium chloride (NaCl) solution and the mixture was stirred for 24 h to allow the H^+ ions to exchange with the Na^+ ions. The released H^+ ions were titrated with 0.1 M sodium hydroxide (NaOH) solution. The I_{EC} was calculated from the consumed NaOH via the following formula:

$$I_{EC} = \frac{\text{consumed NaOH(mL)} \times \text{molarity of NaOH}}{\text{dried polymer weight (g/meq)}} \quad (1)$$

For the measurement of the ionic conductivity, the compressed membrane form of sulfonated PS and the Pt-sulfonated PS fibers were located at the center of the cell with both chambers containing 1 M sulfuric acid (H_2SO_4) solution. The electrode used in the test was Pt black (area = 1 cm × 1 cm) and the electrical resistance (R_1) was measured in the frequency range of 0.1-10^5 Hz at 1 volt using an LCR tester (Reactance Capacitor Resistor tester, Hioki Model 3522 m, Japan). The electrical resistance (R_2) of the 1 M H_2SO_4 solution without a membrane was also measured. The electrical conductivity (σ) of the membrane was calculated by subtracting the value of R_2 from R_1, viz.:

$$\sigma = \frac{d}{(R_2 - R_1)A} \quad (2)$$

where σ is the proton conductivity (S/cm), R is the bulk resistance or ohmic resistance of the membrane sample (ohm), d is the distance between the electrodes (cm), and A is the effective area of the membrane (cm^2).

Fourier transform infrared (FT-IR) measurements were carried out for the PS fibers by means of a Bruker (MCT Mid-IR) spectrometer equipped with attenuated total reflection

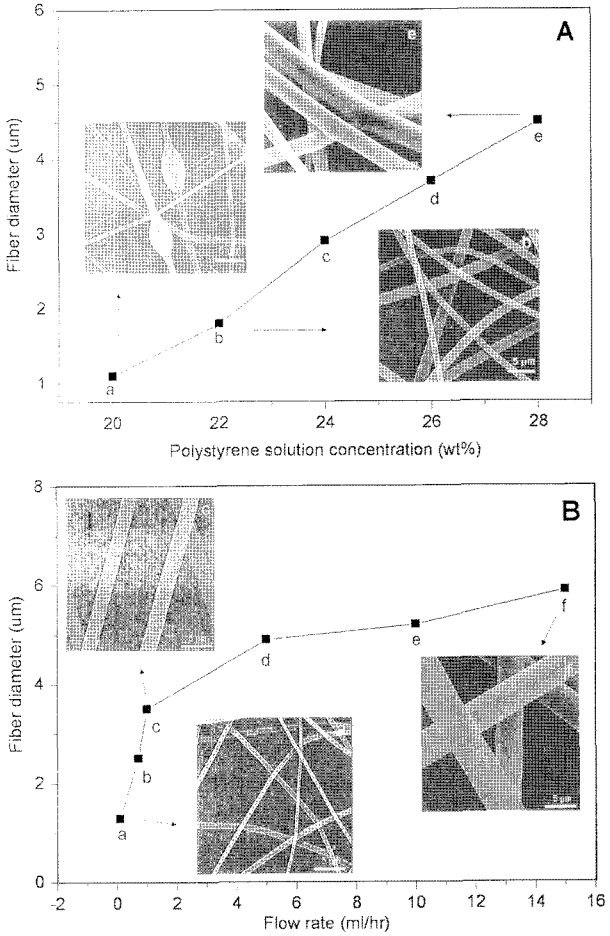

Figure 1. Fiber diameters and SEM images (A) at different PS solution concentrations: (a) 20 wt%, (b) 22 wt%, (c) 24 wt%, (d) 26 wt%, and (e) 28 wt% with 5 mL/h. Fiber diameters and SEM images (B) at various flow rates: (a) 0.1, (b) 0.7, (c) 1, (d) 5, (e) 10, and (f) 15 mL/h at 22 wt%.

(ATR). The spectra were measured in the transmittance mode over the wavenumber range of 4000-700 cm^{-1}. The morphology of the fibers and membranes was examined using scanning electron microscopy (SEM, S-2140, Hitachi, Japan) and transmission electron microscopy (TEM, JEM2100F, JEOL, Japan). An inductively coupled plasma-optical emission spectrometer (ICP-OES, Varian 720-ES, Varian, USA) was used for the quantification of the total Pt loading in the Pt-loaded PS fibers.

Results and Discussion

Figure 1(a) shows the SEM morphology of the electrospun fibers prepared from the PS solutions in DMF with concentrations of 20, 22, 24, 26, and 28 wt%. As can be seen, as the PS solution concentration increases, the fiber diameter also increases. At the lowest concentration of 20 wt%, a straight fiber is not usually formed due to the high surface tension.[44] In addition, no fibers were formed at concentrations over 28 wt% in this study, due to the high solution viscosity.[23] Accordingly, the PS concentration of 22-28 wt% in DMF is considered to be the range of fiber formation in our study. Particularly, the concentration of 22 wt% was considered to be the optimal condition and, thus, unless otherwise stated, a concentration of 22 wt% was used for further analysis in this study.

Figure 1(b) shows the effect of the flow rate on the electrospun fibers, based on flow rates of 0.1, 0.7, 1.0, 5.0, 10.0, and 15.0 mL/h at a fixed PS concentration of 22 wt% using an applied voltage of 10 kV and tip-to-collector distance of 10 cm. As can be seen in Figure 1(b), as the flow rate increases, the fiber diameter also increases. In this study, a flow rate of 0.1 mL/hr was considered to be the most appropriate condition and, thus, unless otherwise stated, the PS fibers were prepared at a flow rate of 0.1 mL/h for the PS solution at 22 wt%.

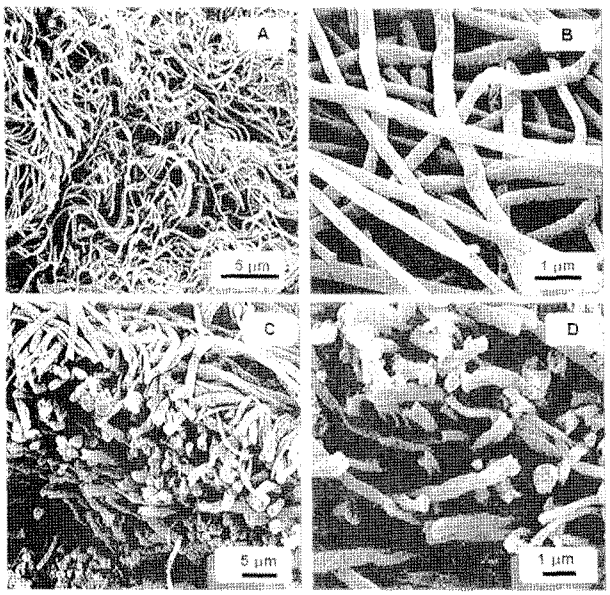

Figure 2. Compression-molded fibrous PS membrane (0.1 mL/h, 22 wt%) sulfonated by chlorosulfonic acid for 0.8 h so as to have an I_{EC} value of 3.0 meq/g, exhibiting the membrane surface (A and B) and the fractured cross-section (C and D) at different magnifications.

Figure 2 shows the surface and cross section of the compressed PS fibers formed via the electrospinning, sulfonation, and room-temperature compression molding processes. It can be seen that the electrospun PS fibers sulfonated by chlorosulfonic acid for 0.8 h so as to have an I_{EC} value of 3.0 meq/g, are mechanically interlocked by the solid-state compression molding process, which results in their containing tightly entangled electrospun fibers. The surface of the compressed fiber bed in Figures 2(A) and (B) reveals the pores formed in the interstitial space of the electrospun fibers. When the compressed fibers were fractured for microscopic observation, the entangled fibers were not elongated or pulled out (Figures 2(C) and (D)), which may indicate that the fiber entanglement is strong enough to maintain its structure. The fiber-entangled pores appear to be a desirable structure for use as a polyelectrolyte porous structure containing cationic selectivity, while the fibrous skeleton structure is sustained.

The typical FT-IR spectra of the pristine PS fibers and the corresponding sulfonated ones (sulfonated by chlorosulfonic acid for 0.8 h with the I_{EC} value of 3.0 meq/g) are compared in Figure 3. The characteristic peak of the aromatic =C-H stretching band of PS is shown at 3026 cm^{-1}. The peak at 2924 cm^{-1} is assigned to the $-CH_2-$ asymmetric stretching band of PS. The sharp peak at 1412 cm^{-1} is assigned to the C=C para-disubstituted benzene band of PS. Before the sulfonation, an aromatic =C-H stretching band at 3026 cm^{-1}, $-CH_2-$ asymmetric stretching band at 2924 cm^{-1}, and C=C para-disubstituted benzene band at 1412 cm^{-1} can be observed. All of these peaks can be seen for both the pristine and sulfonated PS fibers, except for the 1217 cm^{-1} peak, which confirms the presence of the SO_3^- group introduced by sulfonation. After the sulfonation, the intensities of the peaks at 3026, 2924, and 1412 cm^{-1} decrease, while that of the SO_3^- group band at 1217 cm^{-1} increases, demonstrating that the $-CH_2-$, =C-H, and C=C bonds are substituted with the SO_3^- group. As shown in the insets of Figure 3(A), the pristine PS fibers are straight. When the PS fibers are treated with chlorosulfonic acid, the localized heating and swelling of the fibers may well take place. As a result, the inset in Figure 3(B) shows the curved PS fibers due to the residual stresses, which might well be induced during the electrospinning and lamination processes.

The sulfonation of the PS fibers causes the fiber surface to become ion-selective and, consequently, the porous bed composed of sulfonated PS fibers turns into a polyelectrolyte one. The I_{EC} values of the sulfonated PS fibers at the various

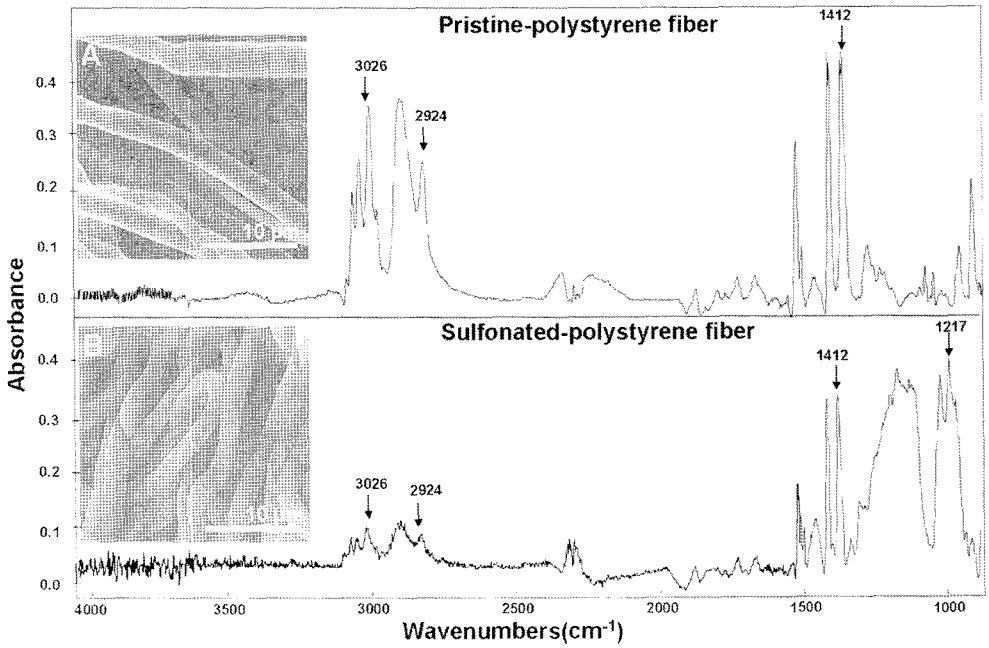

Figure 3. FT-IR spectra of pristine-PS (A) and sulfonated-PS fibers sulfonated by chlorosulfonic acid for 0.8 h so as to have an I_{EC} value of 3.0 meq/g (B).

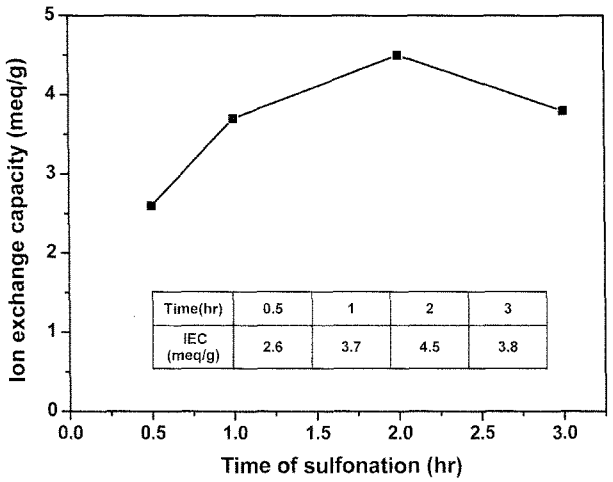

Figure 4. Ion exchange capacity of sulfonated PS membranes measured as a function of the sulfonation time.

sulfonation times are presented in Figure 4, viz. 2.6, 3.7, 4.5, and 3.8 meq/g at 0.5, 1.0, 2.0, and 3.0 h, respectively. These I_{EC} values in our study are relatively high compared with those of other polymer systems such as acid functionalized poly(arylene ether), which provides I_{EC} values of the order of 2.0 meq/g.[45] As can be seen in Figure 4, the extent of sulfonation continuously increases, reaching a maximum after around 2 h of treatment. A similar sulfonation process of PS, which was grafted on poly(vinylidene fluoride) films, was reported, where the sulfonation started at the surface of the PS and then proceeded towards the internal layers by the diffusion of the sulfonating agent, giving a maximum I_{EC}

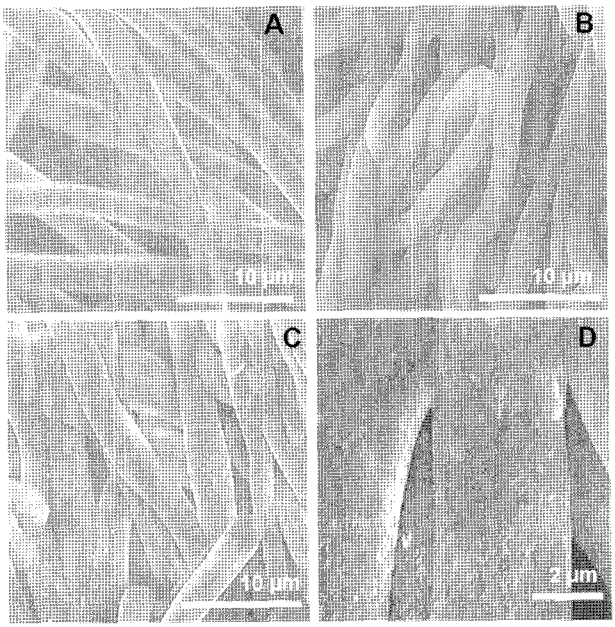

Figure 5. SEM images of pristine-PS fibers (A), sulfonated-PS membranes (B), and Pt-incorporated PS fibers at different magnifications (C and D). All images were taken from the compression-molded membranes.

after 2.0 h of treatment.[46] In this study, the complete sulfonation of our PS fiber system is also achieved after around 2 h of sulfonation.

The scanning electron micrographs in Figure 5 compare the pristine PS fiber (A), the sulfonated one (B), and the Pt-incorporated ones (C and D). The fiber diameters of the

electrospun PS fibers are 3-4 μm for both the pristine and sulfonated PS fibers (having an I_{EC} value of 3.0 meq/g), and the surface appears to be smooth, demonstrating that the fibers are sulfonated without damaging the PS surface morphology. A highly-entangled feature of crooked electrospun fibers can also be seen after the compression molding process in Figures 5(C) and (D). The micrographs of the Pt-loaded PS fibers indicate that the Pt nanostructure is not a spherical shape but a crumpled-sheet shape evenly formed at the fiber surface through the ion interaction of SO_3^- and $Pt(NH_3)_4^{2+}$ ultimately giving Pt^0 by chemical reduction. The Pt entities generated in the vicinity of the counter-charged heterogeneous surface give rise to this unique crumpled sheet shape.

Assuming that the sulfonic acid groups are formed on the PS fiber surface, the number of SO_3^- groups formed on the PS fiber may be estimated using the I_{EC} values.[1] For example, when the I_{EC} value is 3.0 meq/g, the number of SO_3^- groups can be estimated to be 18×10^{20} per g of PS using the following relation, viz.:

$$N_{SO_3^-} = I_{EC} N_A \tag{3}$$

where $N_{SO_3^-}$ is the number of SO_3^- groups per g of PS and N_A is Avogadro's number. The number of ion exchange sites formed on the polymer surface is an absolute measure of the reactive sites available for the ionic metal complex to be metallized. In addition to the I_{EC} value, however, it is believed that steric hindrance may occur in the ionic interaction of the cationic complex with the sulfonic acid groups, due to the limited length of the sulfonated PS repeating unit. In the presence of this steric hindrance, the cationic complex may not be able to interact with all of the available sulfonic acid groups. Scheme I compares the sizes of the Pt cation and the repeating length of SO_3^- in PS. As can be seen, the distance between the three SO_3^- groups in the PS chains is about 5.04 Å, which is comparable to the size of the $Pt(NH_3)_4^{2+}$ ion of around 4.76 Å.[47] Accordingly, it may be reasonable to assume that three SO_3^- groups would interact with one $Pt(NH_3)_4^{2+}$ ion in the ion-exchange reaction. For the estimation of the metal loading content in the *in-situ* metallization method, the number of SO_3^- groups interacting with a single $Pt(NH_3)_4^{2+}$ ion may be defined as the interaction parameter (υ). Then, the weight ratio (R) of platinum to PS fibers can be estimated by the following relation:

$$R = \frac{N_{SO_3^-} M_w}{\upsilon N_A} = \frac{I_{EC} M_w}{\upsilon} \tag{4}$$

where υ is the interaction parameter and M_w is the molecular weight of Pt, viz. 195. In this study, $N_{SO_3^-}$ can be estimated by eq. (3) to be 18×10^{20} per g of PS. If υ is assumed to be 3, R can be estimated by eq. (4) to be 0.195 g of Pt per g of PS which gives the Pt loading, $[R/(1+R)]$, as 16.32 wt%. For comparison, the Pt loading on the sulfonated PS membrane is ca. 15.82 wt%, as measured by ICP-OES, which is in good agreement with the estimated value. According to this result, the Pt loading in our *in-situ* metallization process may be controlled by adjusting the I_{EC} value and the interaction parameter, which is based on the steric arrangement of the interacting ions and ionic groups.

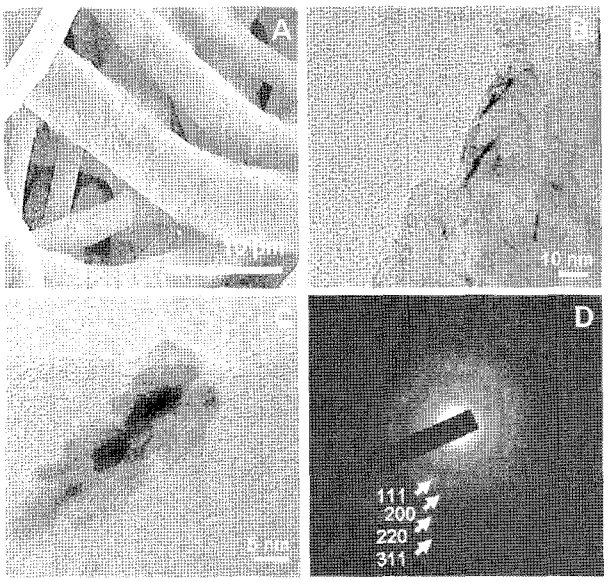

Figure 6. SEM (A) and TEM (B and C) images of platinum formed on the surface of the PS fibers. The electron diffraction ring pattern of Pt is shown in (D).

Table I. The Ionic Conductivity Values of the Pristine PS, Sulfonated PS, and Pt-PS Membrane

Sample	Pristine PS	Sulfonated PS*	Pt-PS*
σ(S/cm)	0.005	0.09	0.32

*Sulfonated by chlorosulfonic acid for 2 h so as to have an I_{EC} value of 4.5 meq/g.

Figure 6 shows the electron micrograph images of the Pt formed on the PS fiber surface. As seen in Figures 6(B) and 6(C), the Pt nanostructure formed by the *in-situ* metallization method exhibits a unique shape resembling a needle and/or crumpled sheet, which is apparently different from a particle or thin film. This seems to be due to the fact that the platinum complex is strongly bound with the sulfonic acid group in ionic form, while being reduced to platinum metal. Figure 6(D) shows the electron diffraction ring pattern of Pt, of which each ring represents the lattice spacing corresponding to the [111], [200], [220], and [311] planes of the fcc platinum.

Finally, the ionic conductivity of the compressed PS fibers is summarized in Table I. The sulfonated PS fibers (2 h of sulfonation with I_{EC} = 4.5 meq/g) and its corresponding Pt-sulfonated PS fibers show ionic conductivities of 0.09 and 0.32 S/cm, respectively, which are well over the ionic conductivity of Nafion of 0.053 S/cm.[20] The increased ionic

conductivity of the Pt-loaded PS fibers is considered to be due to the catalytic activity of the Pt particles in the ion-exchange and diffusion process of cations along the ionic polymer surface. Overall, the membrane form of Pt-loaded PS fibers showed good potential for use as a catalyzed polyelectrolyte system in many electrochemical and catalytic applications, due to its low cost and high conductivity. For example in direct methanol fuel cell applications, the methanol crossover problem may be diminished by the Pt-catalized cation-selective porous media.

Conclusions

Pt-catalyzed polyelectrolyte porous bed was prepared by the electrospinning of PS followed by a solid-state compression method. The PS fibers were sulfonated by chlorosulfonic acid and the surface of the sulfonated PS fibers was metallized with Pt using the *in-situ* metallization method. The compressed PS fiber bed showed cation-selective polyelectrolyte characteristics with ionic conductivities of up to 0.32 S/cm, which could endow the novel hydrocarbon polyelectrolyte system with the capability of oxidizing crossover methanol in direct methanol fuel cells.

Acknowledgement. This work was supported by grant No. R012006000103480 from the Basic Research Program of the Korea Science & Engineering Foundation. We also appreciate the instrumental and technical support from the Samsung Advanced Institute of Technology through SAINT, Sungkyunkwan university.

References

(1) T. H. Han, D. O. Kim, Y. K. Lee, S. J. Suh, H. C. Jung, Y. S. Oh, and J. D. Nam, *Macromol. Rapid Commun.*, **27**, 1483 (2006).
(2) B. C. H. Steele and A. Heinzel, *Nature*, **414**, 345 (2001).
(3) S. M. J. Zaidi and M. I. Ahmad, *J. Membrane Sci.*, **279**, 548 (2006).
(4) J. H. Cho and F. Caruso, *Chem. Mater.*, **17**, 4547 (2005).
(5) O. A. Baturina, S. R. Aubuchon, and K. J. Wynne, *Chem. Mater.*, **18**, 1498 (2006).
(6) J. H. Nam, Y. Y. Jang, Y. U. Kwon, and J. D. Nam, *Electrochem. Commun.*, **6**, 737 (2004).
(7) K. Lee, J. H. Nam, J. H. Lee, Y. Lee, S. M. Cho, C. H. Jung, H. G. Choi, Y. Y. Chang, Y. U. Kwon, and J. D. Nam, *Electrochem. Commun.*, **7**, 113 (2005).
(8) J. H. Lee, J. H. Lee, J. D. Nam, H. R. Choi, K. M. Jung, W. J. Jeon, Y. K. Lee, K. J. Kim, and Y. S. Tak, *Sensors & Actuators A*, **118**, 98 (2005).
(9) N. Kato and F. J. Caruso, *J. Phys.Chem. B*, **109**, 19604 (2005).
(10) J. Mann, N. Yao, and A. B. Bocarsly, *Langmuir*, **22**, 10432 (2006).
(11) E. P. Murray, T. Tsai, and S. A. Barnett, *Nature*, **400**, 649 (1999).
(12) M. A. Hickner, H. Ghassemi, Y. S. Kim, B. R. Einsla, and J. E. McGrath, *Chem. Rev.*, **104**, 4587 (2004).
(13) N. Asano, A. Makoto, S. Suzuki, K. Miyatake, H. Uchida, and M. Watanabe, *J. Am. Chem. Soc.*, **128**, 1762 (2006).
(14) C. H. Rhee, H. K. Kim, H. Chang, and J. S. Lee, *Chem. Mater.*, **17**, 1691 (2005).
(15) Z. Chen, B. Holmberg, W. Li, X. Wang, W. Deng, R. Munoz, and Y. Yan, *Chem. Mater.*, **18**, 5669 (2006).
(16) A. R. Tan, L. M. Carvalho, and A. S. Gomes, *Macromol. Symp.*, **229**, 168 (2005).
(17) P. Xing, G. P. Robertson, M. D. Guiver, S. D. Mikhailenko, and S. Kaliaguine, *Macromolecules*, **37**, 7960 (2004).
(18) S. Swier, V. Ramani, J. M. Fenton, H. R. Kunz, M. T. Shaw, and R. A. Weiss, *J. Membrane Sci.*, **256**, 122 (2005).
(19) C. Genies, R. Mercier, B. Sillion, N. Cornet, G. Gebel, and M. Pineri, *Polymer*, **42**, 359 (2001).
(20) N. Carretta, V. Tricoli, and F. Picchioni, *J. Membrane Sci.*, **166**, 189 (2000).
(21) M. M. Nasef, N. A. Zubir, A. F. Ismail, K. Z. M. Dahlan, H. Saidi, and M. Khayet, *J. Power Sources*, **156**, 200 (2006).
(22) T. Yamaguchi, H. Kuroki, and F. Miyata, *Electrochem. Commun.*, **7**, 730 (2005).
(23) A. Frenot and I. S. Chronakis, *Curr. Opin. Colloid Interface Sci.*, **8**, 64 (2003).
(24) Y. H. Lee, J. H. Lee, I. G. An, C. Kim, D. S. Lee, Y. K. Lee, and J. D. Nam, *Biomaterials*, **26**, 3165 (2005).
(25) S. W. Choi, J. R. Kim, Y. R. Ahn, S. M. Jo, and E. J. Cairns, *Chem. Mater.*, **19**, 104 (2007).
(26) H. Dong, E. Fey, A. Gandelman, and W. Jones, *Chem. Mater.*, **18**, 2008 (2006).
(27) M. Watanabe, H. Uchida, and H. Igarashi, *Macromol. Symp.*, **156**, 223 (2000).
(28) S. J. Lee, S. Mukerjee, J. McBreen, Y. W. Rho, Y. T. Kho, and T. H. Lee, *Electrochim. Acta*, **24**, 3693 (1998).
(29) M. Pan, H. Tang, S. P. Jiang, and Z. J. Liu, *Electrochem. Soc.*, **152**, A1081 (2005).
(30) R. G. Freeman, K. C. Grabar, K. J. Allison, R. M. Bright, J. A. Davis, A. P. Guthrie, M. B. Hommer, M. A. Jackson, P. C. Smith, D. G. Walter, and M. J. Natan, *Science*, **267**, 1629 (1995).
(31) S. Kubo, Z. Z. Gu, D. A. Tryk, Y. Ohko, O. Sato, and A. Fujishima, *Langmuir*, **18**, 5043 (2002).
(32) O. Prucker and J. Ruhe, *Macromolecules*, **31**, 592 (1998).
(33) J. H. Lee, D. W. Kim, G. S. Song, Y. G. Lee, S. B. Jung, and J. D. Nam, *Macromol. Rapid Commun.*, **28**, 634 (2007).
(34) P. A. Schueler, J. T. Ives, F. DeLaCroix, W. B. Lacy, P. A. Becker, J. Li, K. D. Caldwell, B. Drake, and J. M. Harris, *Anal. Chem.*, **65**, 3177 (1993).
(35) A. B. R. Mayer, W. Grebner, and R. Wannemacher, *J. Phys. Chem. B*, **104**, 7278 (2000).
(36) P. Lianos and J. K. Thomas, *J. Colloid Interf. Sci.*, **117**, 505 (1987).
(37) S. Shibata, K. Aoki, T. Yano, and M. Yamane, *J. Sol-Gel Sci. Tech.*, **11**, 279 (1998).
(38) V. G. Pol, D. N. Srivastava, O. Palchik, V. Palchik, M. A. Slifkin, A. M. Weiss, and A. Gedanken, *Langmuir*, **18**, 3352 (2002).
(39) B. Wang, Z. Ji, F. T. Zimone, G. M. Janowski, and J. M. Rigsbee, *Surf. Coat. Technol.*, **91**, 64 (1997).
(40) J. Zhang, J. Liu, S. Wang, P. Zhan, Z. Wang, and N. Ming, *Adv. Funct. Mater.*, **14**, 1089 (2004).

(41) S. L. Westcott, S. J. Oldenburg, T. R. Lee, and N. J. Halas, *Langmuir*, **14**, 5396 (1998).
(42) A. Dokoutchaev, J. T. James, S. C. Koene, S. Pathak, G. K. S. Prakash, and M. E. Thompson, *Chem. Mater.*, **11**, 2389 (1999).
(43) J. P. Shin, B. J. Chang, J. H. Kim, S. B. Lee, and D. H. Suh, *J. Membrane Sci.*, **251**, 247 (2005).
(44) K. H. Lee, H. Y. Kim, H. J. Bang, Y. H. Jung, and S. G. Lee, *Polymer*, **44**, 4029 (2003).
(45) C. K. Shin, G. Maier, and G. G. Scherer, *J. Membrane Sci.*, **245**, 163 (2004).
(46) N. Walsby, M. Paronen, J. Juhanoja, and F. Sundholm, *J. Appl. Polym. Sci.*, **81**, 1572 (2001).
(47) J. S. Casasa, Y. Parajóa, Y. Romeroa, A. Sánchez-Gonzáleza, J. Sordoa, and E. M. Z. Vázquez-Lópezb, *Anorg. Allg. Chem.*, **630**, 980 (2004).